



Nonlinear Amplifier Effect on High Bit Rate Modulation Techniques Used in WiFi Generation with MATLAB Simulink

Fatima Faydhe Al-Azzawi^{1*}, Kamal Y. Kamal^{1,2}, Majida Saud Ibrahim¹, Saba Dhey Abed¹

¹ Institute of Technology, Middle Technical University (MTU), Baghdad 10074, Iraq

² School of Engineering, University of Guelph, Guelph N1G 2W1, Ontario, Canada

Corresponding Author Email: fatima_faydy1981@mtu.edu.iq

Copyright: ©2024 The authors. This article is published by IETA and is licensed under the CC BY 4.0 license (<http://creativecommons.org/licenses/by/4.0/>).

<https://doi.org/10.18280/mmp.110103>

ABSTRACT

Received: 20 July 2023

Revised: 2 September 2023

Accepted: 10 September 2023

Available online: 30 January 2024

Keywords:

high bit rate modulation, M-QAM, nonlinear amplifier, WiFi

High bit rate modulation is an essential aspect of next-generation WiFi and plays a crucial role in achieving high data rates and increased network capacity. High-bit rate modulation uses advanced modulation schemes, such as 4096-QAM, to increase the maximum number of bits sent over a particular frequency band. Using nonlinear amplifiers in wireless communication systems will significantly improve the performance of high bit rate modulation techniques, such as 4096-QAM. Nonlinear amplifiers can cause a range of impairments, including intermodulation, harmonic distortion, and amplitude compression, which can affect the transmitted signal quality. It is essential to minimize the effects of these impairments through proper design and optimization of the amplifier to ensure the highest quality possible of the transmitted signal. In this paper, M-QAM with nonlinear amplifier system design and implanted with MATLAB Simulink where in terms of Transmitted and Received spectrum signal and constellation diagram and calculated error vector magnitude (EVM) and modulation error ratio (MER) measurements for 1024, 2048, and 4096-QAM that used in WiFi 6, WiFi 6E, WiFi 7, respectively.

1. INTRODUCTION

High bit rate modulation is an essential aspect of next-generation WiFi and plays a crucial role in achieving high data rates and increased network capacity. High-bit rate modulation uses advanced modulation schemes, such as 4096-QAM, to increase the number of bits sent over a particular frequency band [1, 2].

One of the key benefits of high bit rate modulation providers is that they make better use of the available spectrum, enabling more data to be sent across a given frequency band. This is crucial since the demand for wireless data is rising and straining the available spectrum [3].

Improved signal quality, enhanced robustness against interference, and dependability in noisy environments are further benefits of high bit rate modulation. This is especially crucial for applications that need to send audio or video in high definition [4, 5].

In the context of next-generation WiFi, high bit rate modulation is especially important because it makes multiple-input multiple-output (MIMO) technology possible, which boosts link capacity and increases spatial multiplexing [6, 7].

Next-generation WiFi must include high bit rate modulation in order to maximize network capacity, improve signal quality, and make better use of the spectrum's resources. Technological advancements in high bit rate modulation are necessary to meet the growing demand for wireless data [8, 9].

In wireless communication systems, high bit rate

modulation schemes like 4096-QAM can perform much better when nonlinear amplifiers are used. The quality of the transmitted signal can be impacted by a number of impairments caused by nonlinear amplifiers, including as amplitude compression, harmonic distortion, and intermodulation [10, 11].

When two or more signals are mixed in a nonlinear amplifier, intermodulation takes place, producing new signals that weren't there before. This may lead to interference, lower the signal-to-noise ratio, and lower the transmitted signal's quality [12].

When an amplifier modifies the transmitted signal's structure, higher-frequency components stand out more, a phenomenon known as harmonic distortion takes place. This may result in worse signal quality and more spectrum spreading [11, 13].

When the amplifier is unable to supply the transmitted signal enough gain, the amplitude is compressed. This phenomenon is known as amplitude compression. As a result, the signal quality and signal-to-noise ratio may decrease [14-20].

These impairments can negatively impact the performance of high bit rate modulation techniques used in WiFi technologies. To minimize these effects, nonlinear amplifiers should be designed and optimized to minimize these impairments, ensuring that the transmitted signal is of the highest quality possible [21-23].

Using nonlinear amplifiers in wireless communication

systems can significantly improve the performance of high bit rate modulation techniques used in WiFi. It is important to minimize the effects of these impairments through proper design and optimization of the amplifier to ensure the highest quality possible transmitted signal [24-28].

In this paper, M-QAM with nonlinear amplifier system design and implanted with MATLAB Simulink where in terms of Transmitted and Received spectrum signal and constellation diagram and calculated error vector magnitude (EVM) and modulation error ratio (MER) measurements for 1024, 2048, and 4096-QAM that used in WiFi 6, WiFi 6E, WiFi 7, respectively.

2. NONLINEAR AMPLIFIER

A nonlinear amplifier is a type of amplifier that amplifies an input signal in a nonlinear manner. Unlike linear amplifiers, which amplify the input signal proportionally, nonlinear amplifiers introduce distortions into the output signal [8, 9].

These distortions can result in intermodulation, harmonic distortion, and amplitude compression, which can negatively affect the quality of the transmitted signal. Nonlinear amplifiers are commonly used in various applications, including communication, power, and audio systems [8, 9].

Reducing the impairments caused by the nonlinear behavior while maintaining the gain and output power required for the application is one of the major problems in constructing nonlinear amplifiers.

Nonlinear amplifiers are frequently used in communication systems to supply the high power and gain needed for wireless transmission. Feedforward linearization and digital pre-distortion are two examples of linearization techniques that are frequently employed to reduce the impairments caused by nonlinear behavior.

To sum up, nonlinear amplifiers introduce distortions into the output signal via amplification of the input signal in a nonlinear manner. The transmitted signal's quality may be negatively impacted by these distortions, thus it's critical to reduce them through appropriate amplifier design and optimization.

There are two viable methods for signals with a vast dynamic range: The simplest is to utilize a programmable gain amplifier (PGA) or a variable gain amplifier (VGA). Using a closed-loop circuit that also measures the signal characteristics, such as its maximum value or RMS (root mean square) under the control of a system processor, these have their gain automatically changed. The VGA/PGA technique is effective in some applications, although it is typically not appropriate for signals with more dynamic range than roughly 10dB. The logarithmic (log) amplifier offers a solution when the dynamic range exceeds what the VGA/PGA can manage. This amplifier uses a straightforward transfer function [10, 11]:

$$V_{out} = K \ln(V_{in}) \quad (1)$$

where, K is a scaling factor.

Three fundamental topologies can be employed, starting with the most straightforward diode log amp. The fundamental voltage-current relationship is logarithmic in a diode. The voltage of inverting op-amp will be proportional to the input current in a log form if a diode is placed in the feedback channel, Figure 1.

The following equations describe the relationship between the input voltage V_{in} and the output voltage V_{out} :

$$V_{out} = -V_T \ln\left(\frac{V_{in}}{I_S R}\right) \quad (2)$$

where, I_S and V_T stand for the diode's thermal voltage and saturation current, respectively.

Due to non-ideal diode characteristics, the design dynamic range is typically only 40-60dB, but if the diode is replaced with diode-connected transistor, as shown in Figure 2, the dynamic range can be increased to 120dB or more.

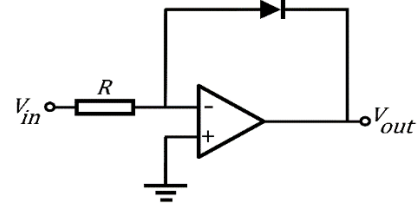


Figure 1. The Diode/Op-amp log amp

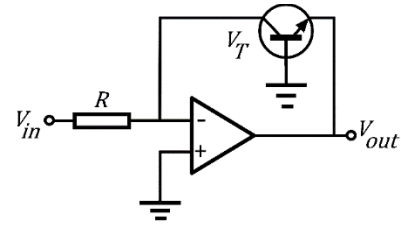


Figure 2. Op-amp log amp with transistor

A log amplifier must always have a positive input voltage, or V_{in} , to function correctly. This can be ensured by conditioning the input signal using a filter rectifier before applying it to the input of the log amplifier. As the op-amp is in the configuration of inverting and V_{in} is positive, V_{out} must be negative and is sufficient to forward bias the emitter-base junction of the BJT, keeping it in the active mode of operation [12, 13]. Now:

$$V_{BE} = -V_{out}$$

$$I_C = I_S (e^{\frac{V_{BE}}{V_T}} - 1) \approx I_S e^{\frac{V_{BE}}{V_T}}$$

$$V_{BE} = V_T \ln\left(\frac{I_C}{I_S}\right) \quad (3)$$

It is the emitter-base diode's saturation current. Due to the op-amp differential input's virtual ground [14, 15]:

$$I_C = \frac{V_{in}}{R}$$

$$V_{out} = -V_T \ln\left(\frac{V_{in}}{I_S R}\right) \quad (4)$$

3. M-QAM MODULATION WITH NONLINEAR AMPLIFIER SIMULINK

M-QAM transceiver design and implanted using MATLAB Simulink as shown in Figure 3, where signal source block

illustrated in Figure 4, starting with Random Integer block that Generate random uniformly distributed integers in the range $[0, M-1]$, where M is the set size. Followed by M-QAM block

Modulate the input signal using the rectangular quadrature amplitude modulation method. This block will receive a column vector or scalar input signal.

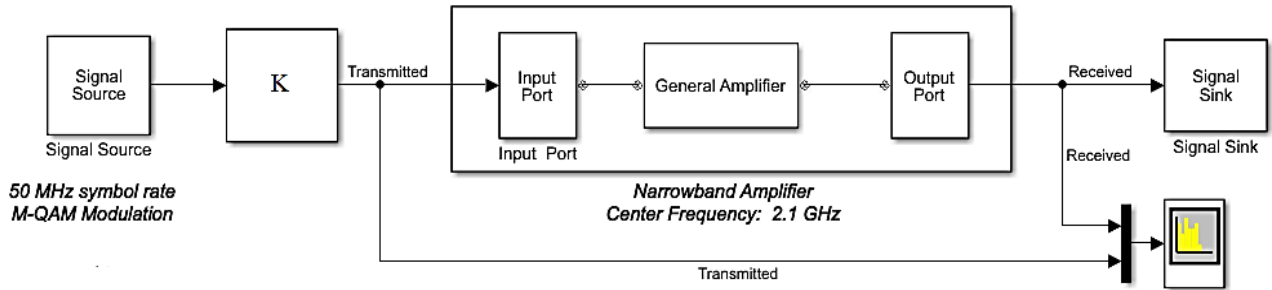


Figure 3. M-QAM modulation with nonlinear amplifier MATLAB Simulink

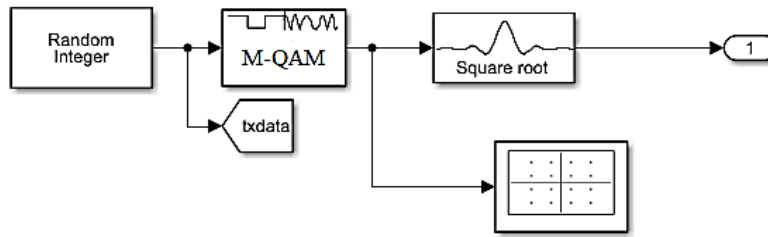


Figure 4. Signal source block

Bits or integers may be used as the input signal. The input width must be an integer multiple of the number of bits per symbol if the “Input type” parameter is set to “Bit”. After that, Raised Cosine transmits the Up-sample and filters the input signal using a regular or square root raised cosine FIR filter. K block is a slide gain block whereby Move the slider modifies the scalar gain. To observe the nonlinear effect in this design, double-click the Slider Gain block and modify the gain value while the model is running [22, 23].

Input Port in the Narrowband Amplifier Connection block from Simulink to RF Block set physical blocks. The RF Block sets physical blocks of a modeling approach using baseband equivalents. This method simulates a $1/(Sample\ time)$ bandwidth, with the center frequency set at the desired value. This frequency value corresponds to 0Hz in the baseband-equivalent model. The block provides the option to interpret the Simulink signal as either the incident power wave to the RF system or the source voltage of the RF system. The ‘Incident power wave’ option is the most common RF modeling interpretation, while the ‘Source voltage’ option is provided for backward compatibility. If the input Simulink signal is the incident power wave, the output of the RF system is the transmitted power wave. If the input is the source voltage, the output is the load voltage.

The block controls the modeling of RF Block set, physical blocks between this block and the Output Port block using:

- FIR filters to model the frequency-dependent characteristics
- Look up tables to model the nonlinear behaviors

Optional guard bands can be specified as a fraction of the modeling bandwidth.

The guards’ bands are implemented by applying a Tukey window to the frequency response. Modeling delay may be added to improve the response of the FIR filters. The parameters of this block are shown in Figure 5.

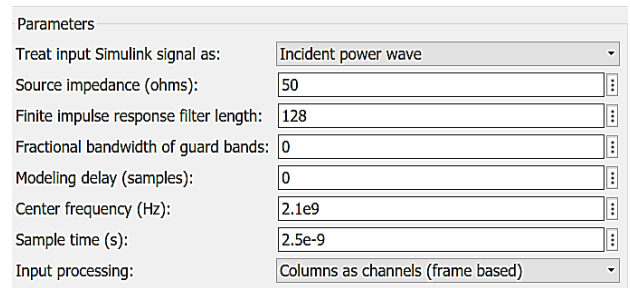


Figure 5. The parameters of the input port of the Narrowband amplifier

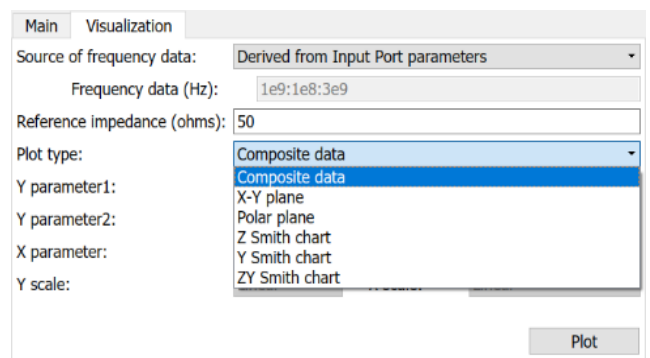


Figure 6. Parameters of output port

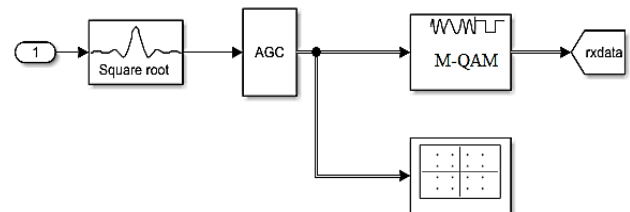


Figure 7. Signal sink block

A general amplifier block is an RF amplifier described by a data source that consists of either an object or data from a file. When there is no noise data in the data source, use the Noise Data tab to specify amplifier noise information. The Noise Data tab accepts a separate N-element vector of the corresponding frequency values for a frequency-dependent noise. When there is no non-linearity data in the data source, use the Non-linearity Data tab to specify amplifier non-linearity information. The Non-linearity Data tab accepts a separate N-element vector of the corresponding frequency values for a frequency-dependent non-linearity. When the data source contains operating condition information, use the Operating Conditions tab to select operating condition settings for the simulation. Data interpolation is used during simulation.

Output Port in Narrowband Amplifier Connection block from RF Block set physical blocks to Simulink. Several RF system characteristics, which are separated by an input port block and an output port block, can be displayed once a simulation has been conducted, including composite data, an X-Y plane, a polar plane, a Z Smith chart, a Y Smith chart, and a ZY Smith chart. as shown in Figure 6.

The signal sink block contains a visa-versa of the signal source, as shown in Figure 7.

4. SIMULINK RESULTS

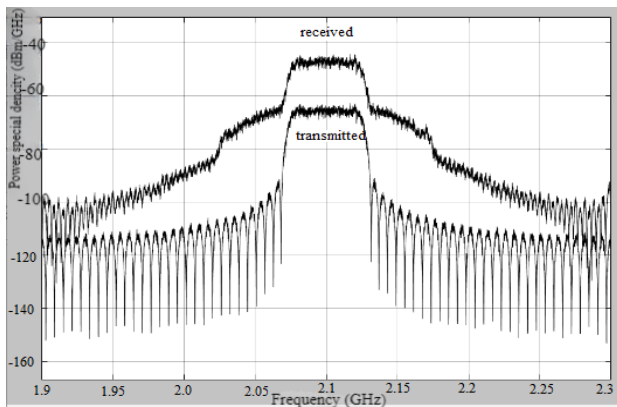


Figure 8. 4096-QAM transmitted and received signals spectrums

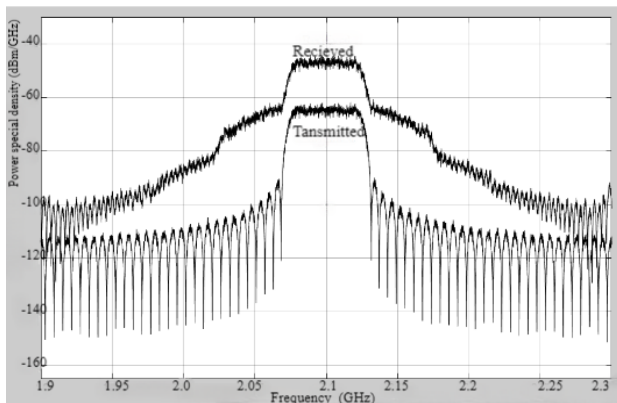


Figure 9. 2048-QAM transmitted and received signals spectrums

M-QAM transceiver design and implanted using MATLAB Simulink as shown in Figure 3, where M used 1024, 20248, and 4096 in WiFi 6, WiFi 6E, and WiFi 7, respectively. When comparing the spectrums of transmitted and received signals,

the spectrum regrowth at the received signal can be seen. This regrowth is due to the amplifier's non-linearity, as shown in Figures 8-10. From these figures, the non-linearity effect on the three M-QAM modulations is equally affection on the spectrum; the percentage of growth from the main loop to the side loop is -65 to -95 dBm/Hz power spectral density in the transmitted signal to -45 to -65 dBm/Hz power spectral density in the received signal.

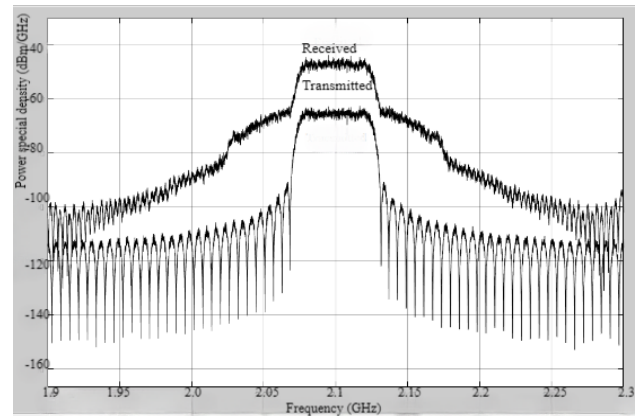


Figure 10. 1024-QAM transmitted and received signals spectrums

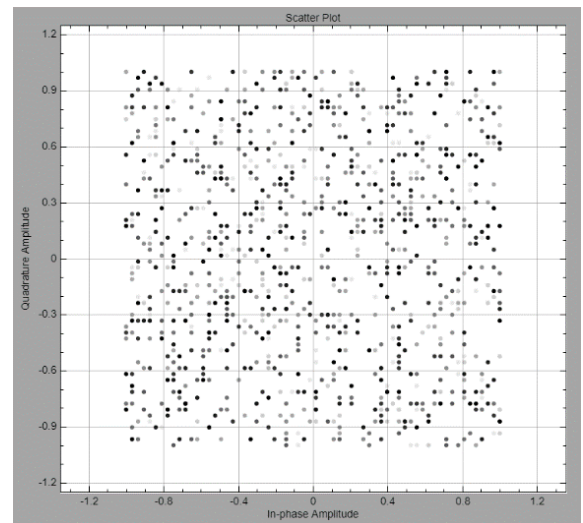


Figure 11. 4096-QAM transmitted signal constellation

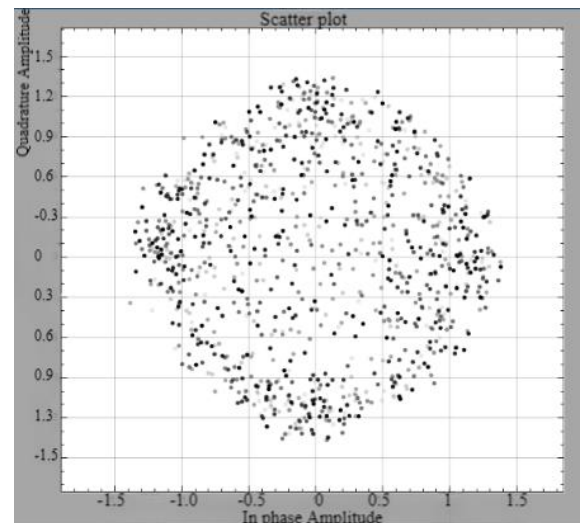


Figure 12. 4096-QAM received signal constellation

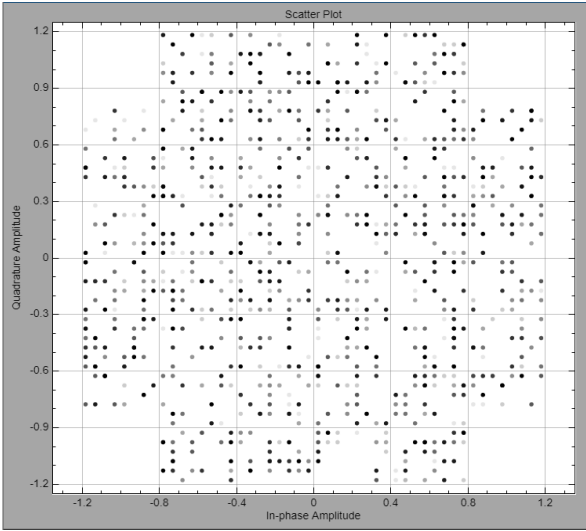


Figure 13. 2048-QAM transmitted signal constellation

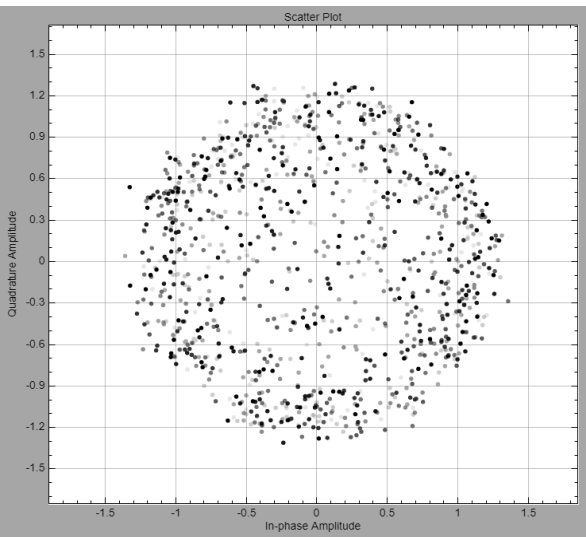


Figure 14. 2048-QAM received signal constellation

When comparing the constellations of transmitted and received signals, Figures 11-16 can be seen as the signal distortion of the received signal. This distortion is due to the non-linearity of the amplifier.

Display calculated error vector magnitude (EVM) and modulation error ratio (MER) measurements in Table 1, where RMS EVM increased by 0.16% at the receiver with 1024-QAM while decreasing by 0.75%, 27% for 2048, 4096-QAM, respectively. Peak EVM increased by 1.52% at the receiver

with 1024-QAM, decreasing by 0.21% and 0.53% at the receiver for 2048 and 4096 QAM, respectively. Avg EVM decreased for all M-QAM by 0.06dB, 0.26dB, and 0.09dB, respectively. Peak EVM decreased by 0.31dB and 0.11dB at the receiver for 1024-QAM and 4096-QAM while increased by 0.05dB at 2024-QAM, Avg MER increased for all types of M-QAM by 1.11dB, 1.15dB, 1.16dB respectively.

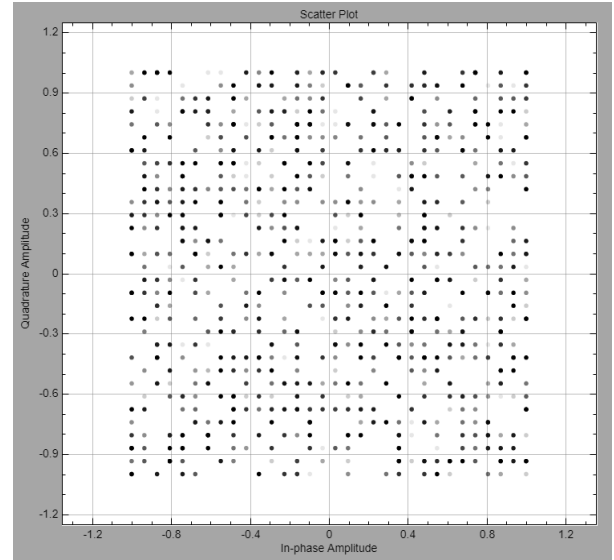


Figure 15. 1024-QAM transmitted signal constellation

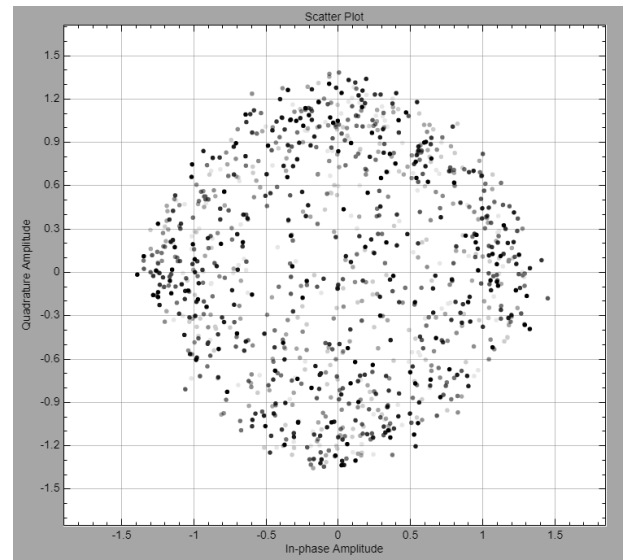


Figure 16. 1024-QAM received signal constellation

Table 1. Error Vector Magnitude (EVM) and Modulation Error Ratio (MER) measurements

EVM/MER	1024-QAM		2048-QAM		4096-QAM	
	Transmitter	Receiver	Transmitter	Receiver	Transmitter	Receiver
RMS EVM (%)	24.67	24.83	25.32	24.57	24.81	24.54
Peak EVM (%)	41.96	43.48	44.08	43.87	42.82	43.35
Avg EVM (dB)	-12.16	-12.10	-11.93	-12.19	-12.11	-12.20
Peak EVM (dB)	-7.54	-7.23	-7.11	-7.16	-7.37	-7.26
Avg MER (dB)	11.15	12.26	11.04	12.19	11.21	12.37

5. CONCLUSION

In this paper, M-QAM with nonlinear amplifier system design and implanted with MATLAB Simulink where in terms

of Transmitted and Received spectrum signal and constellation diagram and calculated error vector magnitude (EVM) and modulation error ratio (MER) measurements for 1024, 2048, and 4096-QAM that used in WiFi 6, WiFi 6E, WiFi 7

respectively, when comparing the spectrums of transmitted and received signals it can be seen the spectrum regrowth at the received signal. This regrowth is due to the non-linearity of the amplifier. The non-linearity effect on the three M-QAM modulations is equally affection on the spectrum. The growth percentage from the main loop to the side loop is -65 to -95 dBm/Hz power spectral density in the transmitted signal to -45 to -65 dBm/Hz power spectral density in the received signal. When comparing the constellations of transmitted and received signals, the signal distortion of the received signal can be seen.

This distortion is due to the non-linearity of the amplifier. Display is the calculated error vector magnitude (EVM) and modulation error ratio (MER) measurements, where RMS EVM increased by 0.16% at the receiver with 1024 QAM while decreasing by 0.75%, 27% at the receiver for 2048, 4096-QAM, respectively. Peak EVM increased by 1.52% at the receiver with 1024 QAM, decreasing by 0.21%, and 0.53% at the receiver for 2048 and 4096 QAM, respectively. Avg EVM decreased for all M-QAM by 0.06dB, 0.26dB, and 0.09dB, respectively. Peak EVM decreased by 0.31dB and 0.11dB at the receiver for 1024 QAM and 4096 QAM while increasing by 0.05dB at 2024 QAM. Avg MER increased for all types of M-QAM by 1.11dB, 1.15dB, and 1.16dB, respectively. From above, the use of nonlinear amplifiers in wireless communication systems can significantly impact the performance of high bit rate modulation techniques, such as 4096-QAM. Nonlinear amplifiers can cause a range of impairments, including intermodulation, harmonic distortion, and amplitude compression, which can affect the quality of the transmitted signal. It is essential to minimize the effects of these impairments through proper design and optimization of the amplifier to ensure that the transmitted signal is of the highest quality possible.

REFERENCES

- [1] Al-Azzawi, F.F., Abid, F.A., Naji, M.K. (2022). Radio frequency receiver of long-term evolution system design by MATLAB Simulink. *Telkomnika (Telecommunication Computing Electronics and Control)*, 20(2): 244-251. <http://doi.org/10.12928/telkomnika.v20i2.20936>
- [2] Al-Azzawi, F.F., Abed, S.D., Ibrahim, M.S. (2022). WiGig WiFi performance with multi-impairment environments in MATLAB Simulink. In 2022 Second International Conference on Advances in Electrical, Computing, Communication and Sustainable Technologies (ICAECT), Bhilai, India, pp. 1-7. <https://doi.org/10.1109/ICAECT54875.2022.9808056>
- [3] Al-Azzawi, F.F., Al-Azzawi, Z.F., Shandal, S., Abid, F.A. (2020). Modulation and RS-CC rate specifications in WiMAX IEEE 802.16 Standard with MATLAB Simulink model. In IOP Conference Series: Materials Science and Engineering. IOP Publishing, 881(1): 012109. <https://doi.org/10.1088/1757-899X/881/1/012109>
- [4] Hidayat, R., Sujana, A., Mahardika, A.G., Herawati, H., Ramady, G.D., Lestari, N.S. (2021). Robust interference cancellation for differential quadrature phase-shift keying modulation with band limiting and adaptive filter. *TELKOMNIKA (Telecommunication Computing Electronics and Control)*, 19(5). <https://doi.org/10.12928/telkomnika.v19i5.19178>
- [5] Al Ibraheemi, H., Al Ibraheemi, M.M. (2020). Wireless communication system with frequency selective channel OFDM modulation technique. *TELKOMNIKA (Telecommunication Computing Electronics and Control)*, 18(3): 1203-1208. <http://doi.org/10.12928/telkomnika.v18i3.14683>
- [6] Al-Azzawi, F.F., Khamees, R.A., Lateef, Z.A., Al-Azzawi, B.F. (2022). Specification of downlink-fixed reference channel DL-FRC for 5G new radio technology. *International Journal of Electrical and Computer Engineering*, 12(1): 453-459. <http://doi.org/10.11591/ijece.v12i1>
- [7] Al-Doori, V.S., Al-Hemiary, E.H. (2020). A simplified spatial Modulation MISO-OFDM scheme. *TELKOMNIKA (Telecommunication Computing Electronics and Control)*, 18(4): 1738-1745. <http://doi.org/10.12928/telkomnika.v18i4.13873>
- [8] Lateef, Z.A., Ibrahim, M.S. (2021). Design and performance thulium doped fiber amplifier in optical telecommunication networks. In *Journal of Physics: Conference Series*. IOP Publishing, 1963(1): 012006. <http://doi.org/10.1088/1742-6596/1963/1/012006>
- [9] He, C., Jiang, H., Chen, D., Geiger, R. (2002). Equivalent gain analysis for nonlinear operational amplifiers. In the 2002 45th Midwest Symposium on Circuits and Systems, 2002. MWSCAS-2002, Tulsa, OK, USA, pp. 1-101. <https://doi.org/10.1109/MWSCAS.2002.1187166>
- [10] Tang, Y., Geiger, R.L. (2002). Effects of open-loop nonlinearity on linearity of feedback amplifiers. In 2002 IEEE International Symposium on Circuits and Systems (ISCAS), Phoenix-Scottsdale, AZ, USA. <https://doi.org/10.1109/ISCAS.2002.1010944>
- [11] Khorov, E., Levitsky, I., Akyildiz, I.F. (2020). Current status and directions of IEEE 802.11 be, the future Wi-Fi 7. *IEEE Access*, 8: 88664-88688. <https://doi.org/10.1109/ACCESS.2020.2993448>
- [12] Hasan, R.J., Abdullah, H.N. (2019). Comparative study of selected subcarrier index modulation OFDM schemes. *TELKOMNIKA (Telecommunication Computing Electronics and Control)*, 17(1): 15-22. <http://doi.org/10.12928/telkomnika.v17i1.10317>
- [13] Hong, W., He, S., Wang, H., Yang, G., Huang, Y., Chen, J., Zhou, J., Zhu, X., Zhang, N., Zhai, J., Yang, L., Jiang, Z., Yu, C. (2018). An overview of China millimeter-wave multiple gigabit wireless local area network system. *IEICE Transactions on Communications*, 101(2): 262-276. <http://doi.org/10.1587/transcom.2017ISI0004>
- [14] Cahyani, R., Perdana, D., Hanuranto, A.T. (2020). A feasibility analysis of the use of IEEE 802.11ah to extend 4G network coverage. *Buletin Pos dan Telekomunikasi*, 18(2): 111-126. <https://doi.org/10.17933/bpostel.2020.180203>
- [15] Suer, M.T., Thein, C., Tchouankem, H., Wolf, L. (2019). Multi-connectivity as an enabler for reliable low latency communications-An overview. *IEEE Communications Surveys & Tutorials*, 22(1): 156-169. <https://doi.org/10.1109/COMST.2019.2949750>
- [16] Yang, M., Li, B., Yan, Z., Yan, Y. (2019). AP coordination and full-duplex enabled multi-band operation for the next generation WLAN: IEEE 802.11 be (EHT). In 2019 11th International Conference on Wireless Communications and Signal Processing (WCSP), Xi'an, China, pp. 1-7.

- <https://doi.org/10.1109/WCSP.2019.8928021>
- [17] Al-Azzawi, F.F., Ibrahim, M.S., Kamal, K.Y. (2023). HaLow Wi-Fi performance in multi-users and channels environment with MATLAB Simulink. *International Journal of Communication Networks and Information Security*, 15(1): 9-15. <https://doi.org/10.17762/ijcnis.v15i1.5487>
- [18] Al Azzawi, F.F., Kamal, K.Y., Qadir, G.A., Abdulghafor, I.A. (2023). LTE transceiver modeling in MATLAB Simulink. In *2023 Third International Conference on Advances in Electrical, Computing, Communication and Sustainable Technologies (ICAECT)*, Bhilai, India, pp. 1-5. <https://doi.org/10.1109/ICAECT57570.2023.10117920>
- [19] Abid, F.A., Al-Azzawi, F.F., Kamal, K.Y., Ibrahim, M.S. (2023). 5G and 6G WiFi transceiver comparison in multi modulation schemes performance with MATLAB Simulink. In *2023 Third International Conference on Advances in Electrical, Computing, Communication and Sustainable Technologies (ICAECT)*, Bhilai, India, pp. 1-7. <https://doi.org/10.1109/ICAECT57570.2023.10117736>
- [20] Al-Azzawi, F.F., Abbas, R.H., Al-Azzawi, Z.F., Kamal, K.Y. (2023). CCDF measurement with Multi Impairment of Wi-Fi 6 performance using MATLAB Simulink. In *2023 Third International Conference on Advances in Electrical, Computing, Communication and Sustainable Technologies (ICAECT)*, Bhilai, India, pp. 1-5. <https://doi.org/10.1109/ICAECT57570.2023.10118293>
- [21] Bankov, D., Khorov, E., Lyakhov, A., Sandal, M. (2019). Enabling real-time applications in Wi-Fi networks. *International Journal of Distributed Sensor Networks*, 15(5): 1550147719845312. <https://doi.org/10.1177/1550147719845312>
- [22] Bankov, D., Didenko, A., Khorov, E., Lyakhov, A. (2018). OFDMA uplink scheduling in IEEE 802.11 ax networks. In *2018 IEEE International Conference on Communications (ICC)*, Kansas City, MO, USA, pp. 1-6. <https://doi.org/10.1109/ICC.2018.8422767>
- [23] Bianchi, G. (2000). Performance analysis of the IEEE 802.11 distributed coordination function. *IEEE Journal on Selected Areas in Communications*, 18(3): 535-547. <https://doi.org/10.1109/49.840210>
- [24] Khorov, E., Kureev, A., Levitsky, I., Akyildiz, I.F. (2020). Prototyping and experimental study of non-orthogonal multiple access in Wi-Fi networks. *IEEE Network*, 34(4): 210-217. <https://doi.org/10.1109/MNET.011.1900498>
- [25] Bellalta, B. (2016). IEEE 802.11 ax: High-efficiency WLANs. *IEEE Wireless Communications*, 23(1): 38-46. <https://doi.org/10.1109/MWC.2016.7422404>
- [26] Kawai, S., Aoyama, H., Ito, R., Shimizu, Y., Ashida, M., Maki, A., Takeuchi, T., Kobayashi, H., Urakawa, G., Hoshino, H., Saigusa, S., Koyama, K., Morita, M., Nihei, R., Goto, D., Nagata, M., Nakata, K., Ikeuchi, K., Yoshioka, K., Tachibana, R., Arai, M., Teh, C.K., Suzuki, A., Yoshida, H., Hagiwara, Y., Kato, T., Seto, I., Horiguchi, T., Ban, K., Takahashi, K., Kajihara, H., Yamagishi, T., Fujimura, Y., Horiuchi, K., Nonin, K., Kurose, K., Yamada, H., Taniguchi, K., Sekiya, M., Tomizawa, T., Taki, D., Ikuta, M., Suzuki, T., Ando, Y., Yashima, D., Kaihotsu, T., Mori, H., Nakanishi, K., Kumagaya, T., Unekawa, Y., Aoki, T., Onizuka, K., Mitomo, T. (2018). An 802.11 ax 4x4 spectrum-efficient WLAN AP transceiver SoC supporting 1024QAM with frequency-dependent IQ calibration and integrated interference analyzer. In *2018 IEEE International Solid-State Circuits Conference-(ISSCC)*, San Francisco, CA, USA, pp. 442-444. <https://doi.org/10.1109/ISSCC.2018.8310374>
- [27] Al-Azzawi, F.F., Khamees, R.A., Ibrahim, M.S., Al-Azzawi, B.F. (2023). Wi-Fi 6 performance in multi modulation scheme with MATLAB Simulink. In *AIP Conference Proceedings*. AIP Publishing, 2591(1). <https://doi.org/10.1063/5.0119335>
- [28] Al-Azzawi, Z.F., Al-Azzawi, F.F., Abid, W.F., Al-Azzawi, B.F. (2023). High bit rate modulation approach used by new generation mobile technology. In *AIP Conference Proceedings*. AIP Publishing, 2591(1). <https://doi.org/10.1063/5.0119336>